

The OTELO survey.

Ángel Bongiovanni^{1,2,3}, on behalf of the OTELO Team

¹ Instituto de Astrofísica de Canarias (IAC), E-38200 La Laguna, Tenerife, Spain

² Departamento de Astrofísica, Universidad de La Laguna (ULL), E-38205 La Laguna, Tenerife, Spain

³ Asociación Astrofísica para la Promoción de la Investigación, Instrumentación y su Desarrollo, ASPID, E-38205 La Laguna, Tenerife, Spain

Abstract

The evolution of galaxies across the cosmic time are observationally studied by means of extragalactic surveys that cover significant volumes of Universe, with a wealth of multi-wavelength ancillary data. OTELO survey provides the deepest narrow band survey to date, in terms of minimum detectable flux, and emission line equivalent width, that has allowed detecting the faintest extragalactic emission line systems. In this way, OTELO data complements other broad band, narrow band, and spectroscopic surveys. The data has been obtained using the red Tunable Filter of the OSIRIS instrument at the 10.4 m telescope GTC, pointing at the most deeply explored EGS region. This catalogue is complemented with public data ranging from deep X-ray to FIR, including high resolution HST images, that allowed deriving precise photometric redshifts, and obtaining the morphological classification of the extragalactic objects detected. In the present contribution the final catalogue and other value-added products, that will be publicly available by mid 2019, are presented. The improved reduction techniques, the high astrometric and photometric quality achieved, and the main survey demographics are also presented. A total of 11 237 raw sources have been detected in a sky area of 56 sq.-arcmin. Within them, about 1 800 are fair candidates to the strongest emission lines in the UV-optical domain, 81 are candidates to stars, while other 483 are candidates to be absorption line systems. The 50% completeness of OTELO catalogue is obtained at an AB magnitude of 26.38. Photometric redshifts have been derived with an accuracy better than $|\Delta z|/(1+z) \leq 0.2$ for 6 600 sources.

1 Introduction

Tracing the star formation rate (SFR) in the Universe along the cosmic eras, as well as the detailed study of the large diversity of activity modes in galaxies, are fundamental science

drivers of the modern extragalactic astronomy. For these purposes, the systematic discovering of emission-line sources (ELS) with increasingly fainter luminosities becomes an essential task. Modern narrow-band and spectroscopic surveys with large aperture telescopes provide large collections of these sources, which facilitate both the follow-up of individual ones as the statistical study of their fundamental properties. In particular, they allow the construction of accurate SFR-line indicator functions, which contribute to a better knowledge of the star formation history of the Universe, and provide valuable constraints to the current models of galaxy evolution.

OTELO (OSIRIS Tunable filter Emission-line Object¹) is a very deep, 2D spectroscopic survey designed primarily for the search of galaxies with emission lines and the measurement of their fluxes and equivalent widths (EW), through the exploitation of the red tunable filter (TF) of the OSIRIS instrument [7]. OTELO obtains spectra of all sources in the field only limited by flux and spectral range, searching for emission lines at different cosmological volumes between redshifts 0.4 and 6, and thereby providing valuable data for tackling a wide variety of science projects, which include the evolution of star formation density up to redshift ~ 1.5 , an approach to the demographics of low-luminosity emission-line galaxies and detailed studies of emission-line ellipticals in the field, high- z QSO, Lyman- α emitters, and Galactic emission-line stars [8].

OTELO shares characteristics of those surveys for the search of emission-line sources, based on spectral scans that use narrow band filters of fixed cavity, such as COMBO-17 [34], ALHAMBRA [22], SHARDS [25], or J-PAS [1], or those that use filters with variable cavity such as TTF [2], CADIS [19] and more recently GLACE [31], or the slit-less spectroscopic surveys limited by the PSF of the system as KISS [33], UCM [15], CUYS [3], and PEARS [32]. However, the data products of OTELO also can be used for a classical narrow-band ELS selection approach [6] from color-magnitude diagrams, such as the described in [24], HIZELS [16], or the surveys compiled in the framework of the HSC-SSP [18]. This possibilities makes OTELO a versatile ELS-finding machine. As most of the mentioned explorations for the search of faint ELS, OTELO will also provide useful predictions for the planning of future surveys (e.g.) DESI [13], PFS [30] or 4MOST-WAVES [12], and space missions like Euclid² or WFIRST-ATLAS [10] that will use these sources as tracers of the large-scale structure.

2 Survey description

OTELO targets a region of the Extended Groth Strip (EGS) embedded in the Deep field 3 of the Canada–France–Hawaii Telescope Legacy Survey³ (CFHTLS) and the deepest pointing of GALEX in imaging and spectroscopy, among other ancillary data which include public images from WIRDS⁴, source catalogues from Chandra [26], *Spitzer*-IRAC and MIPS 24 μm , *Herschel*-PACS 100, 160 μm and -SPIRE 250, 300, 500 μm , as well as spectroscopic redshifts up to $r_{\text{AB}}=24.1$ from DEEP2 [23]. The relative position of the OTELO field in the framework

¹<http://www.iac.es/proyecto/otelo>

²<http://sci.esa.int/euclid/>

³<http://www.cfht.hawaii.edu/Science/CFHTLS>

⁴http://terapix.iap.fr/rubrique.php?id_rubrique=261

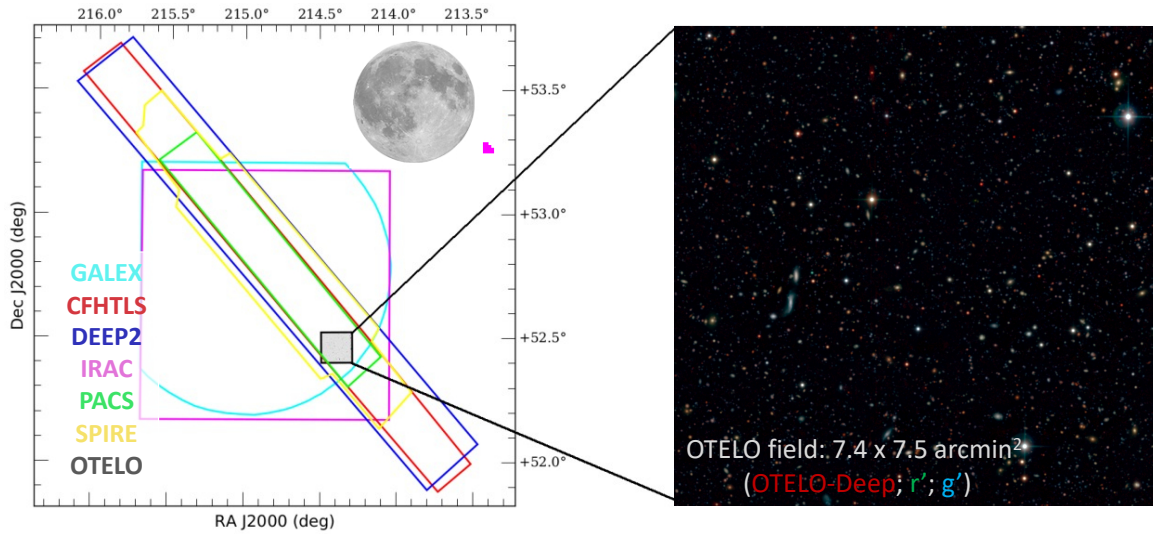


Figure 1: Relative position of the OTELO field together with the UV, optical, IR, and spectroscopic data imprints in the Extended Groth Strip region (left). The RBG composition at right expands the surveyed area represented ($7.5 \times 7.4 \text{ arcmin}^2$) and it is a coadding of the OTELO TF scans (i.e. OTELO-Deep image) combined with the resampled CFHTLS r' - and g' -band images.

of complementary surveys in the EGS is shown in Figure 1.

OTELO was conceived as a narrow band spectral scan (resolution $R \simeq 700$), defined in a window of 230 \AA , centred at 9175 \AA , between two airglow Meinel bands. Hence, the scan is embedded in the SDSS z -band response. The main part of the survey consisted of a tomography of 36 slices evenly distributed in the the wavelength range defined above. A TF width (FWHM) of 12 \AA was adopted, scanning every 6 \AA . This sampling is close to the best equilibrium between a reasonable observing time and the deblending of the $H\alpha$ from the $[\text{NII}]6548,6584$ emission lines ([20]). A total of 108 dark hours (net integration time: 6 600 s/slice), under a guaranteed gime (GT) agreement⁵, distributed over four campaigns between 2010 and 2014, were used for gathering the TF raw data.

The physics behind the TF is the same as the interference filters that are commonly used in astronomy, but with the versatility given by the possibility to control the width of the resonant cavity and, therefore, the wavelength of filter response for a given interference order. The particular characteristics and calibration details of the OSIRIS TF are well studied and can be looked up in [17] and additional references given in the GTC URL⁶.

The TF data was properly reduced using both standard and ad-hoc procedures designed for removing sky rings and image fringing. After flux and wavelength calibrations of TF data, two products emerged: (i) a raw catalogue of 11 237 sources detected in the synthesis of the TF individual images (i.e. the OTELO-Deep image), and (ii) an equal number of *pseudo-*

⁵Defined between the OSIRIS Instrument Team and the Instituto de Astrofísica de Canarias.

⁶<http://www.gtc.iac.es/instruments/osiris/osiris.php>

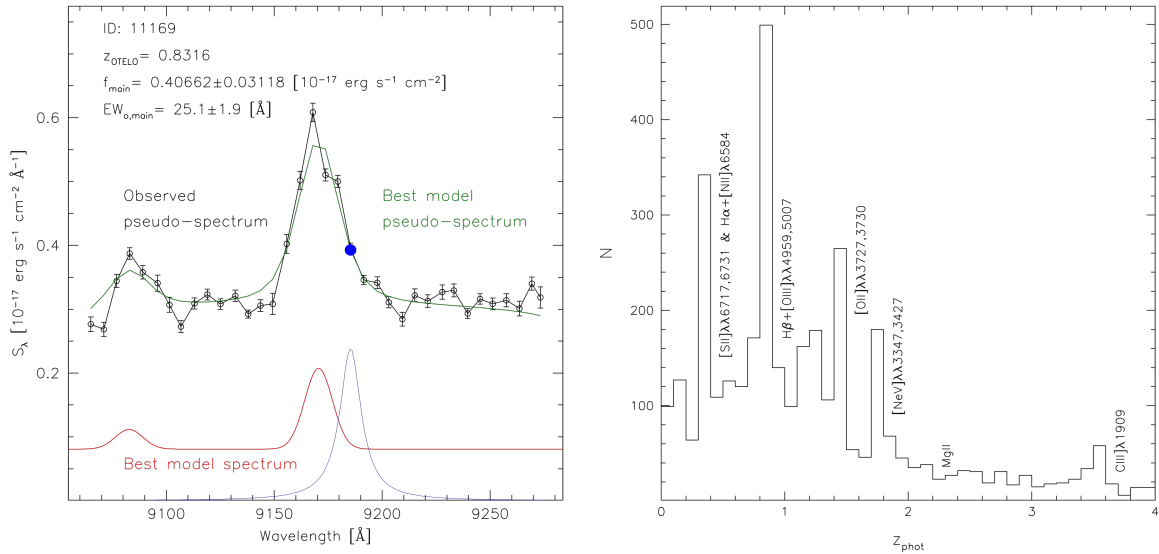


Figure 2: Left: example of a pseudo-spectrum corresponding to a [OIII] ELS at $z=0.8316$ (black dots). The convolution of the best model spectrum is the best fit of the observed data. The blue curve is the TF transmission of the slice corresponding to the blue dot. Right: photometric redshift distribution of the OTELO sources up to $z=4$.

spectra. Unlike the spectra obtained by diffraction devices, in a pseudo-spectrum the SED of a given source is convolved in the wavelength space by the TF instrumental response. An example of a real pseudo-spectrum from OTELO data is given in Figure 2 (left panel). Sources that show two or more consecutive slices with a flux excess $\geq 2\sigma$ above the measured background in the OTELO pseudo-spectra are defined as preliminary ELS candidate. Under this criterion, and taking into account the basic parameter space (i.e. line flux, line profile width, flux density at the continuum) of the survey, as well as the measurements of real noise in the TF scan images, we carried out educated simulations ([27, 5]) for modeling the ELS detection probability function. The results of these simulations are useful to predict (e.g.) the emission-line limiting flux and the completeness profiles for specific ELS subsamples.

3 The OTELO database

In order to obtain reliable photometric redshifts for labelling the spectral feature(s) in pseudo-spectra, the availability of the observed SED distributions of the OTELO sources is mandatory. This is also true for the spectral classification of these sources and the estimation of the stellar mass and gas metallicity, among other parameters. The OTELO-Deep image was used not only for obtaining an integrated flux (limiting magnitude $AB=26.4$ at 50% completeness), but also as a detection image to measure broad-band fluxes of the sources (via PSF-matched photometry) in the registered/resampled optical and near-infrared (NIR)

ancillary images from the CFHTLS and WIRDS. The base catalogue obtained in this way was carefully cross-correlated with complementary data mentioned above, giving rise to the OTELO *multi-wavelength catalogue*.

The OTELO photometric redshifts were determined using libraries for Hubble-sequence and starburst galaxies, Seyferts, QSOs, and star templates, including M, L and T dwarfs. The accuracy of the photometric compared to high quality spectroscopic redshifts from DEEP2 is better than $|\Delta z|/(1+z) \leq 0.2$. Hence, the OTELO catalogue has 9 709 sources with non-null photo-z solutions, and 6 600 of them have an uncertainty $\delta z < 0.2(1+z)$. From the latter subset, the right panel of Fig. 2 shows the photo-z distribution of all preliminary ELG candidates up to $z=4$. As expected, most prominent features in this histogram correspond to the strongest emission lines in the optical, summing up about 1 500 candidates. On the other hand, the high-redshift raw subsample is composed by more than 300 candidates. The detailed analysis of these sources is a part of the on-going and forthcoming works.

The OTELO multi-wavelength catalogue, including the best photometric redshifts, the pseudo-spectra, and the cross-references with other catalogs, constitute the database of the survey. Further details about the survey planning, the TF data reduction and calibration, as well as the construction of the OTELO database, can be found in the survey description article [4]. The essential OTELO products and a Web-based tool for data visualization will be publicly released on mid 2019.

4 First results

Apart from the survey presentation, several contributions account for the first scientific exploitation of the OTELO survey. Some of these works start from the general census of the ELS candidates. For instance, the first analysis of the [OIII]4959,5007 ELS at $z\sim 0.9$ [5] yields that OTELO reaches line flux limits $\approx 5 \times 10^{-19} \text{ erg s}^{-1} \text{ cm}^{-2}$, and observed EW in the order of the TF scan sampling (Fig. 3, left panel). We have adopted these values as the characteristic ones of the whole survey and they are consistent with the predictions obtained from the simulations described above. This sensitivity translates to the faint-end of the LF[OIII] (Fig. 3, right panel). Even though OTELO have nothing to say about the bright side, mainly because the effects of the cosmic variance (which force to adopt a mean L^* value), the faint-end can be sampled up to a luminosity of $\log L_{[\text{OIII}]} [\text{erg s}^{-1}] \sim 39$, in a region of the diagram about 25 to 100 times fainter than the lowest luminosity observed through the most recent narrow-band surveys, at the same redshift [21, 11, 18]. Accordingly, OTELO is sampling a population of star-forming galaxies with stellar masses between 10^7 and $\sim 10^{11} M_{\odot}$, most of them compact and disk-like sources.

The results described above are qualitatively consistent with those obtained by [28] from the analysis of the $\text{H}\alpha + [\text{NII}]$ ELS subset at redshift $z\sim 0.4$. In this case, the SFR function obtained extends the faint-end in ~ 1 dex the ensemble of the most recent data given in literature. This work also includes a prescription about the increasing AGN-host contribution with the $\text{H}\alpha$ luminosity at this redshift. About the latter sources, a first inventory of AGN hosts identified in OTELO at redshift $z < 3$, through different diagnostics, is given in [29].

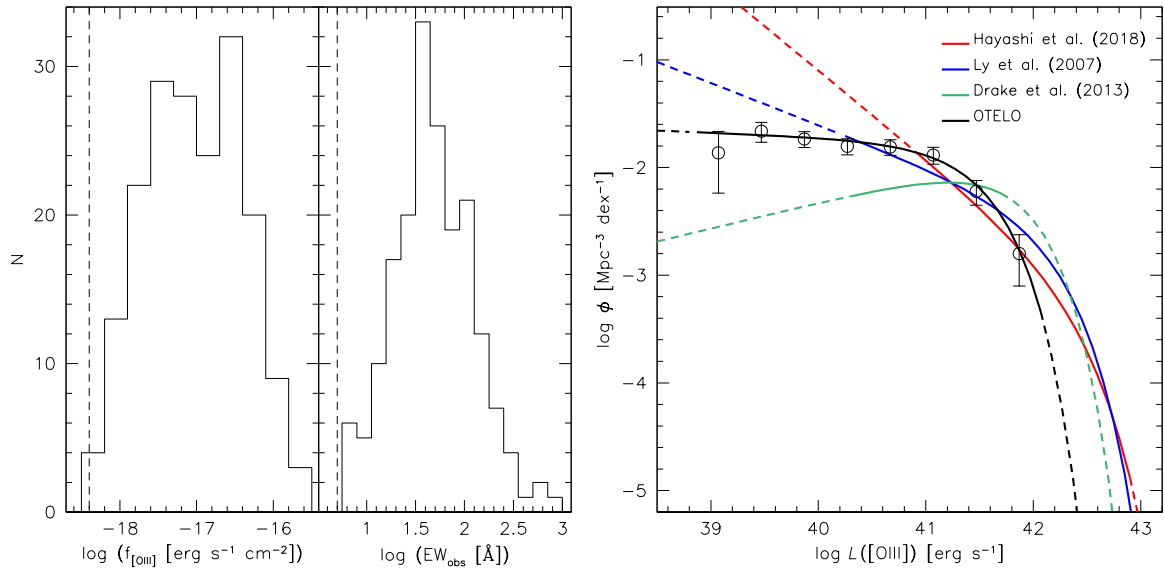


Figure 3: Left: line flux and equivalent width distribution of the OTELO [OIII] ELS sample. Dashed lines are the corresponding limits obtained from ad-hoc simulations of detection probability. Right: luminosity function (LF) of the OTELO [OIII] ELS as given in [5]. Dashed segments are Schechter LF extrapolations from fitted data.

On the other hand, the morphological analysis of the galaxy population in OTELO up to redshift ~ 2 is being currently developed. This analysis is providing clues for additional interpretations of the stellar mass-gas metallicity relation (MZR) for the $H\alpha + [\text{NII}]$ ELS subsample, using the $\text{EW}\alpha\text{n}2$ optical diagnostic diagram given in [9] (see the contribution of J. Nadolny in these Proceedings).

Finally, it is worth pointing out that the OTELO survey is also a very deep probe of the Milky Way halo. The analysis of its stellar component is being carried out. In particular, a cross-correlation with GAIA-DR1 [14] and CFHTLS data has yielded 16 possible emission line stars from a collection of 81 low-mass star candidates (see the contribution of E. Alfaro in these Proceedings).

5 Summary

The OSIRIS tunable filter emission-line survey (OTELO) was designed for the search of ELS by pushing the Gran Telescopio Canarias and this instrument at the limit of their technical capabilities. In this sense, OTELO is detecting ELS with line fluxes as low as $\approx 5 \times 10^{-19} \text{ erg s}^{-1} \text{ cm}^{-2}$ and observed $\text{EW} > 5 \text{ \AA}$. Therefore, OTELO goes one step beyond the conventional spectroscopic surveys and without their selection biases, despite the small sky area (50 arcmin²) and spectral range (230 \AA) explored. These facts confirm the initial expectations of the project, demonstrating the success of the TF tomography technique for

this kind of surveys.

First science exploitation of OTELO was focused on the analysis of the $H\alpha+[NII]6584$ and $[OIII]4959,5007$ ELS at $z\sim 0.4$ and 0.9 , respectively, as well as the first inventory of AGN hosts. Ongoing efforts are being devoted to the analysis of other ELS subsets, as well as in the morphology classification of all sources detected at $z<2$, and the analysis of Galactic halo stars in the field explored.

The OTELO survey is the first large program of GTC whose products will be publicly released on mid 2019.

Acknowledgments

This work was supported by the Spanish Ministry of Economy and Competitiveness (MINECO) under the grants AYA2013-46724-P, AYA2014-58861-C3-1-P, AYA2014-58861-C3-2-P, AYA2014-58861-C3-3-P, AYA2016-75808-R, AYA2016-75931-C2-2-P, AYA2017-88007-C3-1-P and AYA2017-88007-C3-2-P. Based on observations made with the Gran Telescopio Canarias (GTC), installed in the Spanish Observatorio del Roque de los Muchachos of the Instituto de Astrofísica de Canarias, on the island of La Palma. This study makes use of data from AEGIS, a multi-wavelength sky survey conducted with the Chandra, GALEX, Hubble, Keck, CFHT, MMT, Subaru, Palomar, Spitzer, VLA, and other telescopes and supported in part by the NSF, NASA, and the STFC. Based on observations obtained with MegaPrime/MegaCam, a joint project of CFHT and CEA/IRFU, at the Canada-France-Hawaii Telescope (CFHT), which is operated by the National Research Council (NRC) of Canada, the Institut National des Science de l'Univers of the Centre National de la Recherche Scientifique (CNRS) of France, and the University of Hawaii. This work is based in part on data products produced at Terapix available at the Canadian Astronomy Data Centre as part of the Canada-France-Hawaii Telescope Legacy Survey, a collaborative project of the NRC and CNRS. Based on observations obtained with WIRCam, a joint project of the CFHT, Taiwan, Korea, Canada, France, at the Canada-France-Hawaii Telescope (CFHT) which is operated by the National Research Council (NRC) of Canada, the Institut National des Sciences de l'Univers of the Centre National de la Recherche Scientifique of France, and the University of Hawaii. This work is based in part on data products produced at TERAPIX, the WIRDS (WIRcam Deep Survey) consortium, and the Canadian Astronomy Data Centre.

References

- [1] Benítez, N., Dupke, R., Moles, M., et al., 2014, arXiv 1403.5237B
- [2] Bland-Hawthorn, J., & Jones, D. H. 1998, PASA, 15, 44
- [3] Bongiovanni, A., Bruzual, G., Magris, G., et al. 2005, MNRAS, 359, 930
- [4] Bongiovanni, A., et al. 2018a, A&A, forthcoming
- [5] Bongiovanni, A., et al. 2018b, A&A, submitted (under 2nd. revision)
- [6] Bunker, A. J., Warren, S. J., Hewett, P. C., & Clements, D. L. 1995, MNRAS, 273, 513
- [7] Cepa, J., et al. 2003, SPIE, 4841, 1739
- [8] Cepa, J., Bongiovanni, A., Pérez García, A. M., et al. 2013, RMxAC, 42, 70
- [9] Cid Fernandes, R., Stasińska, G., Schlickmann, M. S., et al. 2010, MNRAS, 403, 1036

- [10] Content, R., Wang, Y., Roberto, M., et al. 2018, *Space Telescopes and Instrumentation 2018: Optical, Infrared, and Millimeter Wave*, 10698, 106980I
- [11] Drake, A. B., Simpson, C., Collins, C. A., et al. 2013, *MNRAS*, 433, 796
- [12] Driver, S. P., Davies, L. J., Meyer, M., et al. 2016, *The Universe of Digital Sky Surveys*, 42, 205
- [13] Eisenstein, D., & DESI Collaboration 2015, *American Astronomical Society Meeting Abstracts #225*, 225, 336.05
- [14] Gaia Collaboration, Brown, A. G. A., Vallenari, A., et al. 2016, *A&A*, 595, A2
- [15] Gallego, J., Zamorano, J., Rego, M., et al., 1993, *Astronomische Gesellschaft Abstract Series*, No. 8, p. 39
- [16] Geach, J. E., Smail, I., Best, P. N., et al. 2008, *MNRAS*, 388, 1473
- [17] González, J. J., Cepa, J., González-Serrano, J. I., Sánchez-Portal, M. 2014, *MNRAS*, 443, 3289
- [18] Hayashi, M., Tanaka, M., Shimakawa, R., et al. 2018, *PASJ*, 70, S17
- [19] Hippelein, H., Maier, C., Meisenheimer, K., et al. 2003, *A&A*, 402, 65
- [20] Lara-López, M. A., Cepa, J., Castañeda, H., et al. 2010, *PASP*, 122, 1495
- [21] Ly, C., Malkan, M. A., Kashikawa, N., et al. 2007, *ApJ*, 657, 738
- [22] Moles, M., Benítez, N., Aguerri, J. A. L., et al., 2008, *AJ*, 136, 1325
- [23] Newman, J. A., Cooper, M. C., Davis, M., et al. 2013, *ApJS*, 208, 5
- [24] Pascual, S., Gallego, J., & Zamorano, J. 2007, *PASP*, 119, 30
- [25] Pérez-González, P.G., Cava, A., Barro, G., et al., 2013, *ApJ* 762, 46
- [26] Pović, M., Sánchez-Portal, M., Pérez García, A. M., et al. 2009, *ApJ*, 706, 810
- [27] Ramón-Pérez, M. 2017, *Study of Active Galactic Nuclei in the OTELO survey*. Universidad de La Laguna. PhD thesis
- [28] Ramón-Pérez, M., et al. 2018a, *A&A*, accepted
- [29] Ramón-Pérez, M., et al. 2018b, *A&A*, submitted (under 2nd. revision)
- [30] Takada, M., Ellis, R. S., Chiba, M., et al. 2014, *PASJ*, 66, R1
- [31] Sánchez-Portal, M., Pintos-Castro, I., Pérez-Martínez, R., et al. 2015, *A&A*, 578, A30
- [32] Straughn, A.N., Pirzkal, N., Meurer, G.R., et al. 2009, *AJ*, 138, 1022
- [33] Wegner, G., Salzer, J.J., Jangren, A., et al. 2003, *AJ*, 125, 2373
- [34] Wolf, C., Meisenheimer, K., Rix, H.-W., et al. 2003, *A&A*, 401, 73